



Universiteit
Leiden
The Netherlands

Design and synthesis of NLR and TLR based ligand-antigen conjugates

Willems, M.M.J.H.P.

Citation

Willems, M. M. J. H. P. (2012, November 1). *Design and synthesis of NLR and TLR based ligand-antigen conjugates*. Retrieved from <https://hdl.handle.net/1887/20082>

Version: Corrected Publisher's Version

License: [Licence agreement concerning inclusion of doctoral thesis in the Institutional Repository of the University of Leiden](#)

Downloaded from: <https://hdl.handle.net/1887/20082>

Note: To cite this publication please use the final published version (if applicable).

Chapter 7

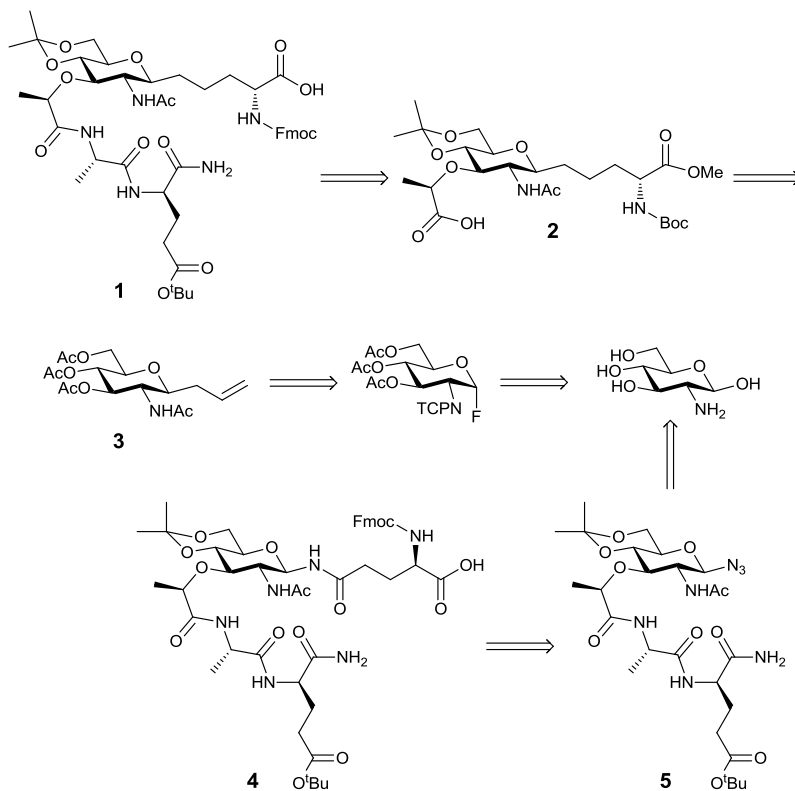
Summary and future prospects

The mammalian immune system protects, amongst others, against invading pathogens and consists of an innate and adaptive component. The innate system is the first line of defense in which pattern recognition receptors (PRRs), especially located on the cell membrane and in the cytosol of antigen presenting cells, detect pathogen associated molecular patterns (PAMPs) that are specific for pathogens. PAMPs exhibit a broad structural variety and the exact molecular structures of ligands that bind to the corresponding PRRs are mostly unknown. Relevant examples of PRRs of which some structurally defined ligands are known, are represented by NOD1, NOD2 and TLR2, TLR4, TLR7 and TLR9. The research presented in this Thesis is directed to the design, synthesis and immunological evaluation of new NOD1, NOD2 and TLR2 ligands as well as conjugates in which these ligands are covalently bound to an antigenic peptide.

Chapter 1 presents an introduction of the reported knowledge about the TLR2 and NOD1, NOD2 receptors with a focus on the associated ligands. Examples of the structure activity studies of the NOD1, NOD2 and TLR2 ligands are discussed. Furthermore, conjugates in which PRR ligands are covalently bound to peptide and carbohydrate antigens are presented.

Chapter 2 informs on the synthesis and immunological evaluation of conjugates in which the NOD2-L MDP is covalently bound to the OVA-derived epitope. In the conjugates the position of attachment of a spacer containing MDP derivative and the antigenic peptide are varied. MDP is connected to the C- or N-terminus of the peptide epitope at its anomeric position or isoglutamic acid. All conjugates were constructed using an automated solid phase peptide synthesis approach giving the pure conjugates in overall moderate yields. The moderate yields can partly be explained by the hydrolysis of the spacer containing MDP derivative during the acidic conditions required for removal of the protective groups and cleavage of the conjugates from the solid support. Introduction of acetyl esters at the 4-*O*- and 6-*O*-positions in the D-glucosamine moiety of MDP increases the stability of the anomeric appendage but did not completely abolish the hydrolysis.

It is proposed to use alternative MDP ligands, having a stable anomeric linkage by replacement of the *O*-glycosidic by a C-glycosidic bond. Retro-synthetic analysis shows that C-glycosidic MDP **1** can be obtained by a condensation of C-glycoside **2** with the dipeptide, described in **Chapter 2** (*Scheme 1*). C-glycoside **2** in turn can be prepared *via* C-glycoside **3** starting from D-glucosamine according to a literature procedure by Fuchss and Schmidt.¹ Introduction of an amide bond, as present in MDP derivative **4**, can also provide the necessary stability. Transformation of D-glucosamine into azide **5** permits subsequent peptide couplings with any amino acid of interest.²

Scheme 1. Retro-synthesis of C-glycosidic MDP (**1**) or MDP derivative **4**.

Another possibility to suppress the acid catalyzed hydrolysis of the anomeric acetal en route to MDP ligands and conjugates is based on the finding that replacement of the 2-*N*-acetyl in MDP by other acyl groups does not hamper the binding capacity to the NOD receptor. To increase the anomeric stability it is proposed to replace the 2-*N*-acetyl in MDP by the electron withdrawing *N*-trifluoroacetyl to give MDP derivative **6** (Figure 1).

Evaluation of the NOD2 based conjugates described in **Chapter 2** showed a confined immunological profile: the cytokine production in the different assays was low but the level of antigen presentation was good. This result indicates that to improve the immunological properties of these conjugates a more potent NOD2 ligand is requested while the conjugation method can stay intact.

To obtain more potent NOD2 ligands, several lipophilic MDP derivatives were synthesized and evaluated for their immunological stimulatory capacity as reported in **Chapter 3**. Fatty acids were placed on the C-6 position or on the anomeric spacer of the D-glucosamine moiety of MDP. In addition another lipophilic ligand was obtained by acylation of the lysine that was appended to the peptide part of MDP. These adjustments gave the desired enhanced cytokine production in an assay with a NOD2 specific cell line and in a DC maturation assay. Thereafter the C-6 modified MDP derivative, being the most potent ligand, was connected to the antigenic OVA-derived peptide with the aid of 'click' chemistry to give lipophilic NOD2-L-antigen conjugate with an immunological profile close to the established Pam₃CSK₄-DEVA₅K conjugate.

Guided by the group of Coulomb, who reported the favorable influence of a *N*-glycolyl substituent in MDP on NOD2 activation, it is proposed to synthesize *N*-glycolyl MDP derivative **7** (Figure 1), and incorporate this derivative in a conjugate.³

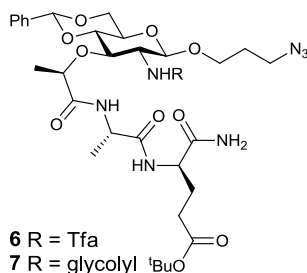


Figure 1. Protected MDP derivative **6** and **7**.

Chapter 4 describes the synthesis and immunological evaluation of a set of bis-conjugates in which both a NOD2-ligand and TLR2-ligand are covalently bound to the OVA-derived epitope. Four different types of conjugates were prepared that differ in the attachment of the NOD2 and TLR2 ligands to C- and N-termini of the peptide epitope. For two types of bis-conjugates the nature of the linker between the ligands and the epitope was varied to avoid the acid catalyzed hydrolysis of MDP during the synthesis and to examine further the influence of the linker on the immunological properties of the conjugates.

All synthesized bis-conjugates responded positive on the NOD2 specific cell assay, a TLR2-knock out assay and a DC maturation assay, meaning that both

receptors are correctly activated by the bis-conjugates. In addition, the induced antigen presentation reached the same level as obtained with the corresponding mono-conjugates. However, the bis-conjugates lacked additive or synergistic effects. Contrary to the nature of the linker, the attachment position of the ligand to the epitope has an effect on the immunological properties of the bis-conjugates: the best results are obtained with the TLR2-L on the C-terminus and NOD2-L on the N-terminus of the epitope. To complete the types of bis-conjugates the synthesis and evaluation of conjugates such as **9** with both MDP and Pam₃CSK₄ on the C-terminus of the epitope (*Figure 2*) is proposed.



Figure 2. Interesting NOD2/TLR2 bis-conjugate **9**.

Since it is largely unknown how PRR ligands and their corresponding conjugates are internalized and subsequently processed in antigen presenting cells, it is proposed to address these issues by the evaluation of conjugates provided with biodegradable linkers such as conjugates with a disulfide linker (**10**) or cathepsin specific cleavable linker (**11 – 14**) between the ligand, Pam₃CSK₄, and the antigenic peptide (*Figure 3*). Depending on the mode of internalization of these conjugates into the cells, the ligand and epitope can be separated in a specific cell compartment and subsequently processed individually. It is anticipated that the disulfide function in conjugate **10** is cleaved by the reductive conditions in the endosome while the oligopeptide linkers in conjugates (**11 – 14**) are cleaved by the proteases cathepsin D, S or E that are located in the cytosol and endoplasmatic reticulum. Stable analogues of the conjugates, in which L-amino acids are replaced by D-amino acids in the linkers of conjugates (e.g. **14**) are needed as reference compounds.

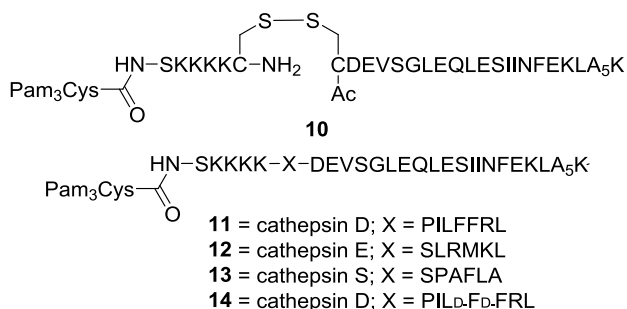
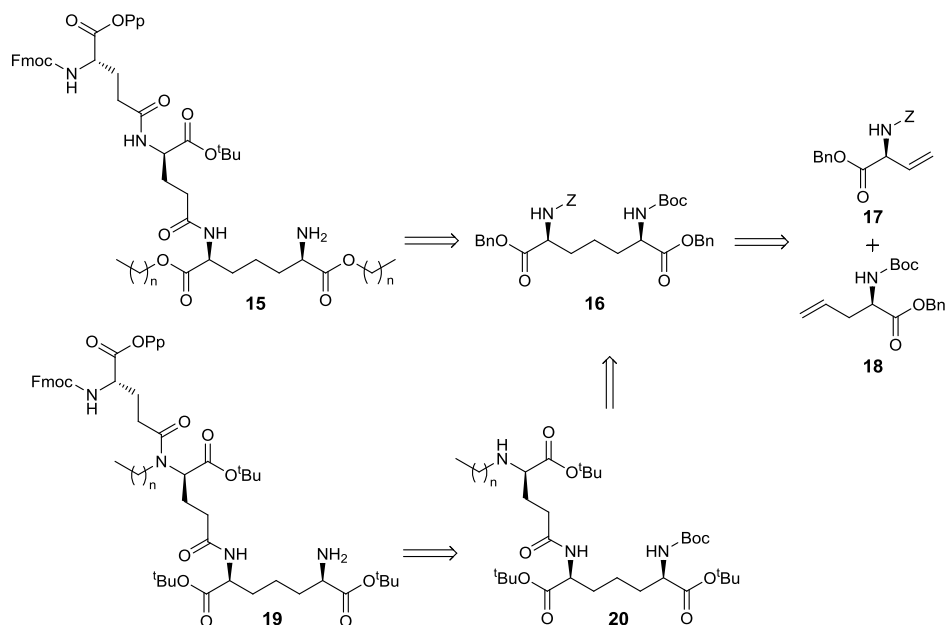


Figure 3. TLR2-L conjugates **10 – 14** with cleavable linkers.

Chapter 1 shows an example of a carbohydrate based antigen cluster covalently bound to a TLR2 ligand that resulted in a potent immune response.⁴ Oligovalent conjugates comprising MUC1 glycopeptides ‘clicked’ to a TLR2 ligand proved to have improved immunostimulatory properties in comparison with the corresponding monovalent conjugates.⁵ Fukase *et al.* revealed that PG sequences (MDP with or without elongation of a lysine or alanine) affected the potency of the constructs more than the number of repeating units of the carbohydrate chain.^{6,7} As shown in **Chapter 4**, a 1 : 1 ratio of ligand and epitope in a conjugate did not result in an enhanced potency. Possibly a cluster of MDP molecules resembling the natural PG carbohydrate chain may lead to an increased immunological response.

Chapter 5 deals with the synthesis and evaluation of mono- and bis-conjugates in which the NOD1 ligand *iE*-DAP as a stereoisomeric mixture is incorporated. Mono-conjugates with the NOD1 ligand *iE*-DAP at the *N*- and *C*-terminus of the epitope were not recognized by the NOD1 receptor and did not induce DC maturation. On the other hand the single NOD1 ligands *iE*-DAP and C12-*iE*-DAP do show NOD1 recognition. It is of interest to synthesize and evaluate orthogonal protected (2*S*,6*R*)-DAP **16** and corresponding mono- and bis-conjugates for which it is proposed to prepare **16** from orthogonal protected vinyl (**17**) and allyl glycine (**18**) *via* a cross metathesis and reduction of obtained double bond (*Scheme 2*). With (2*S*,6*R*)-DAP (**16**) in hands, the chemistry described in **Chapter 2 – 4** can be used to prepare building block **15** and synthesize and evaluate all possible mono- and bis-conjugates.

Enhancement of the lipophilicity of NOD1 ligands can improve the immunological profile, presumably by improved uptake.⁸ This agrees with the finding described in **Chapter 5** that *N*-terminal modified NOD1 ligand C12-*iE*-DAP was more potent than *iE*-DAP. It is suggested to modulate the lipophilicity of building block **15** by varying the alkyl chain (*n*) of the esters.⁹ As an alternative NOD1 derivative compound **19**, accessible from compound **20** is proposed.

Scheme 2. Retro-synthesis of SPPS building blocks **15** and **19** from vinyl and allyl glycine **17** and **18**.

The final **Chapter 6** is devoted to an urea-modification of the established TLR2 ligand Pam₃CSK₄. UPam₃CSK₄, designed with the aid of a crystal structure of the TLR1/2 heterodimer co-crystallized with the Pam₃CSK₄ ligand, proved to be slightly more potent than Pam₃CSK₄. In an attempt to further improve the immunostimulatory activity, the serine residue in UPam₃CSK₄ was replaced by various natural and non-natural amino acids. Substitution with 2-aminobutanoic acid (**X2**), allylglycine (**X5**) or propargylglycine (**X7**) and diaminobutyric acid (**X8**) were most promising in terms of the TLR2 activation (*Figure 4*).

In a preliminary study the influence of the length of the lipophilic tails UPam₃CSK₄ on the activation of TLR2 was studied. There is evidence that the number ($n = 2$ or 3) and length of fatty acids on the glycerol and *N*-terminus of the cysteine in Pam_nCSK₄ determine not only the binding to either the TLR1/2 or TLR2/6 heterodimer but also influence the level of activity.^{10,11} A library consisting of UPam₃CSK₄ derivatives, in which the length of the alkyl chain at the *N*-terminus of cysteine was varied, was prepared (*Figure 4* and experimental details). The promising UPam₃CSK₄ derivatives (described in **Chapter 6**), namely 2-aminobutanoic acid (**X2**) and propargylglycine (**X7**) together with alanine (**X19**), beta-cyanoalanine (**X20**) and 2,3-diaminopropionic acid (**X21**) as other relevant serine substitutions were selected to install lipophilic tails with a chain length of 9, 11 and 13 carbon atoms (*Figure 4*). The corresponding Pam₃Cys derivatives, having fatty acids with the same chain length were prepared as control

compounds. It is of interest to synthesize and to test similar Pam₂Cys derivatives since literature indicates that Pam₂Cys peptides can be more potent than Pam₃Cys peptides.¹²

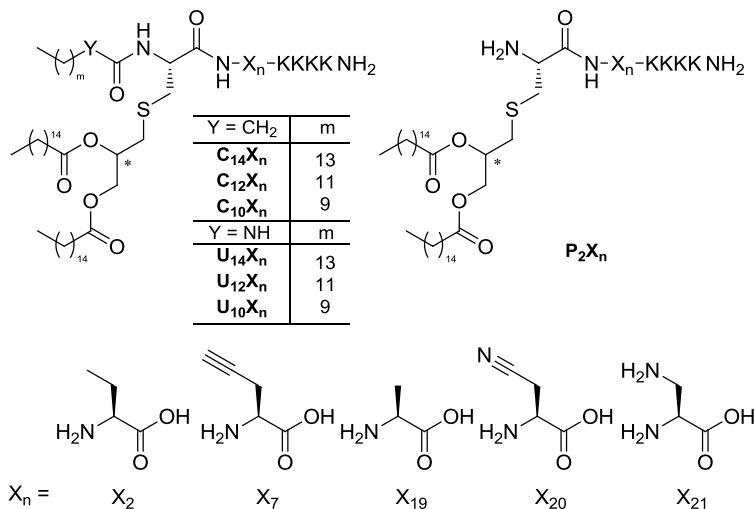


Figure 4. Library 2 with X_n = **X2**, **X7**, **X19**, **X20**, **X21**.

The next step in the immunological evaluation of UpamX_nK₄ derivatives is the incorporation of these ligands in conjugates. In a first experiment, a conjugate of UPam₃X₁SK₄ (X₁ = serine) and antigenic peptide DEVA₅K showed a slightly better DC maturation and a similar antigen presentation in comparison with the parent Pam₃CSK₄-DEVA₅K conjugate. Guided by this finding four novel X₂-modified conjugates were prepared (*Figure 5*), the evaluation of which is in progress.

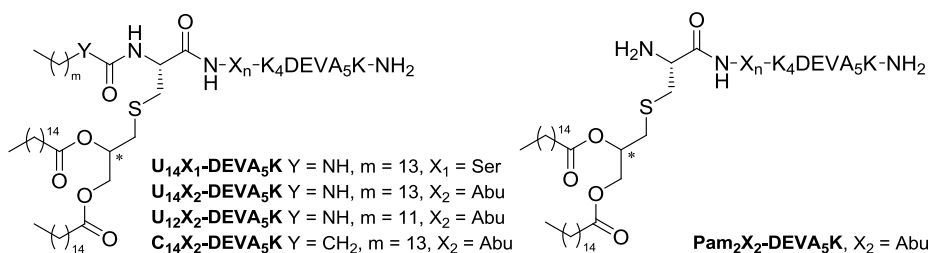


Figure 5. Urea-derived TLR2-L-antigen conjugates.

Most of the processes of the mammalian immune system are not fully understood at molecular level. The TLR2, NOD1 and NOD2 ligands and the associated conjugates with the OVA-derived epitope described in this Thesis, contribute to the insight in these processes. Further elucidation of PRR activation and antigen presentation may eventually result in synthetic vaccine modalities.

Up to now murine assays are used for the immunological evaluation of the compounds, described in this Thesis. In the near future assays with human DCs and possibly *in vivo* studies are planned.

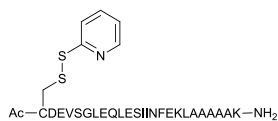
7.2 Experimental

For detailed information on the SPPS of TLR2-conjugates see **Chapter 2 – 4**.

Pam₃Cys-Ser-Lys-Lys-Lys-Lys-Cys-NH₂

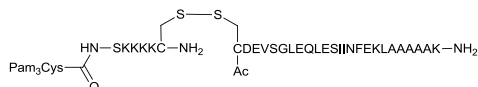
Peptide synthesis was performed on a 50 μmol scale applying the Fmoc based protocol starting from Rink Amide S Tentagel (loading 0.23 mmol/g) ending the synthesis with a final Fmoc deprotection. On 25 μmol scale of crude resin a PyBOP coupling with Palmitoyl-Cys((RS)-2,3-di(palmitoyloxy)-propyl)-OH was performed. Treatment with a cleavage cocktail, precipitation and purification by RP-HPLC yielded title compound. LC/MS: Rt = 7.38 (Alltima CN, 10 – 90% MeCN, 15 min run); ESI-MS: m/z 1613.19 $[\text{M}+\text{H}]^+$; HRMS Calcd. $[\text{C}_{84}\text{H}_{162}\text{N}_{12}\text{O}_{13}\text{S}_2 + \text{H}]^+$ 1613.19321, found 1613.19203.

Ac-Cys(Pys)-Asp-Glu-Val-Ser-Gly-Leu-Glu-Gln-Leu-Glu-Ser-Ile-Ile-Asn-Phe-Glu-Lys-Leu-Ala-Ala-Ala-Ala-Ala-Lys-NH₂¹³



Peptide synthesis was performed on a 50 μmol scale (Rink Amide S Tentagel, loading 0.23 mmol/g) based on standard Fmoc SPPS protocol with a Fmoc deprotection step as final synthesis step. The resin was treated with a cleavage cocktail TFA/TIS/ H_2O (95/2.5/2.5) and 20 eq 2,2'-dithio-bis(pyridine). The solution was filtered and precipitated with Et_2O . Purification yielded LC/MS: Rt = 9.86 min (Alltima C_{18} , 10 – 90% MeCN, 15 min run); ESI-MS: m/z 2801.4, $[\text{M}+\text{H}]^+$.

Pam₃Cys-Ser-Lys-Lys-Lys-Lys-Cys(NH₂)-S-S-(Ac)Cys-Arg-Leu-Asp-Glu-Val-Ser-Gly-Leu-Glu-Gln-Leu-Glu-Ser-Ile-Ile-Asn-Phe-Glu-Lys-Leu-Ala-Ala-Ala-Ala-Ala-Lys-NH₂ (10)



$\text{Pam}_3\text{Cys-Ser-Lys-Lys-Lys-Lys-Cys-NH}_2$ (2 μmol , mg) was dissolved in DMF (2mL) and combined with $\text{Ac-Cys(Pys)-Asp-Glu-Val-Ser-Gly-Leu-Glu-Gln-Leu-Glu-Ser-Ile-Ile-Asn-Phe-Glu-Lys-Leu-Ala-Ala-Ala-Ala-Ala-Lys-NH}_2$ which was dissolved in NH_4OAc (2mL, 1M, pH 6). The resulting mixture was stirred at r.t. for 30 minutes. The mixture was diluted with HOAc (1:1 ratio), checked by LCMS and purified by semi preparative Alltima CN column on the Gilson HPLC system resulting 0.55 mg (6.4%, 0.13 μmol). C/MS: Rt = 6.32 min (Alltima C_{18} , 10 – 90% MeCN, 15 min run); ESI-MS: m/z 4301.5, $[\text{M}+\text{H}]^+$; HRMS Calcd. $[\text{C}_{201}\text{H}_{353}\text{N}_{42}\text{O}_{53}\text{S}_3 + \text{H}]^{3+}$ 1434.85510, found 1434.52005.

Pam₃Cys-Ser-Lys-Lys-Lys-Lys-Pro-Ile-Leu-Phe-Phe-Arg-Leu-Asp-Glu-Val-Ser-Gly-Leu-Glu-Gln-Leu-Glu-Ser-Ile-Ile-Asn-Phe-Glu-Lys-Leu-Ala-Ala-Ala-Ala-Ala-Lys-NH₂ (11)

6 mg (7%, 1.8 μmol); LC/MS: Rt = 8.25 min (Alltima CN, 10 - 90% MeCN, 15 min run); ESI-MS: m/z 4926.05 $[\text{M}+\text{H}]^+$; HRMS Calcd. $[\text{C}_{240}\text{H}_{409}\text{N}_{49}\text{O}_{57}\text{S} + \text{H}]^+$ 1642.68788, found 1642.35481.

Pam₃Cys-Ser-Lys-Lys-Lys-Lys-Gly-Ser-Pro-Ala-Phe-Leu-Ala-Asp-Glu-Val-Ser-Gly-Leu-Glu-Gln-Leu-Glu-Ser-Ile-Ile-Asn-Phe-Glu-Lys-Leu-Ala-Ala-Ala-Ala-Ala-Lys-NH₂ (12)

0.7 mg (0.5%, 0.13 μmol); LC/MS: Rt = 7.50 min (Alltima CN, 10 - 90% MeCN, 15 min). ESI-MS: m/z 4681.84 $[\text{M}+\text{H}]^+$; HRMS Calcd. $[\text{C}_{224}\text{H}_{384}\text{N}_{46}\text{O}_{58}\text{S} + \text{H}]^{3+}$ 1171.21443, found 1171.46659.

***Pam₃Cys-Ser-Lys-Lys-Lys-Lys-Ser-Leu-Arg-Met-Lys-Leu-Asp-Glu-Val-Ser-Gly-Leu-Glu-Gln-Leu-Glu-Ser-Ile-Ile-Asn-Phe-Glu-Lys-Leu-Ala-Ala-Ala-Ala-Lys-NH₂* (13)**

10.6mg (7.6%, 1.9 μmol). LC/MS: Rt = 6.97 min. (Alltima CN, 10 - 90% MeCN, 15 min run); ESI-MS: *m/z* 4766.94 [M+H]⁺; HRMS Calcd. [C₂₂₅H₃₉₉N₄₉O₅₇S₂ + H]³⁺ 1589.65247, found 1589.65515.

Experimental UpamXK₄ Library

For detailed description see Experimental section of Chapter 6.

C14X2, Palmitoyl-Cys((RS)-2,3-di(palimitoyloxy)-propyl)-Abu-Lys-Lys-Lys-Lys-NH₂

0.87 mg (0.58 μmol, 6%); LC/MS: Rt = 8.94 min (Vidac C₄, 50 - 90% MeCN, 15 min run); ESI-MS: *m/z* 1509.19 [M+H]⁺; HRMS Calcd for [C₈₂H₁₅₉N₁₀O₁₁S + H]⁺ 1507.20140, found 1507.20281.

C14X7, Palmitoyl-Cys((RS)-2,3-di(palimitoyloxy)-propyl)-Pra-Lys-Lys-Lys-Lys-NH₂

0.19 mg (0.12 μmol, 1%); LC/MS: Rt = 8.61 min (Vidac C₄, 50 - 90% MeCN, 15 min run); ESI-MS: *m/z* 1517.19 [M+H]⁺; HRMS Calcd for [C₈₃H₁₅₇N₁₁O₁₁S + H]²⁺ 759.09651, found 759.09658.

C14X19, Palmitoyl-Cys((RS)-2,3-di(palimitoyloxy)-propyl)-Ala-Lys-Lys-Lys-Lys-NH₂

0.89 mg (0.60 μmol, 6%); LC/MS: Rt = 8.80 min (Vidac C₄, 50 - 90% MeCN, 15 min run); ESI-MS: *m/z* 1493.19 [M+H]⁺; HRMS Calcd for [C₈₁H₁₅₇N₁₁O₁₁S + H]⁺ 1493.18575, found 1493.18695.

C14X20, Palmitoyl-Cys((RS)-2,3-di(palimitoyloxy)-propyl)-CNAIa-Lys-Lys-Lys-Lys-NH₂

0.42 mg (1.0 μmol, 10%); LC/MS: Rt = 8.63 min (Vidac C₄, 50 - 90% MeCN, 15 min run); ESI-MS: *m/z* 1518.18 [M+H]⁺; HRMS Calcd for [C₈₂H₁₅₆N₁₂O₁₁S + H]⁺ 1518.18100, found 1518.19015.

C14X21, Palmitoyl-Cys((RS)-2,3-di(palimitoyloxy)-propyl)-Dap-Lys-Lys-Lys-Lys-NH₂

0.5 mg (0.33 μmol, 3%); LC/MS: Rt = 7.58 min (Vidac C₄, 50 - 90% MeCN, 15 min run); ESI-MS: *m/z* 1508.20 [M+H]⁺; HRMS Calcd for [C₈₁H₁₅₈N₁₂O₁₁S + H]⁺ 1508.19665, found 1508.19739.

P2X2, Cys((RS)-2,3-di(palimitoyloxy)-propyl)-Abu-Lys-Lys-Lys-Lys-NH₂

2.09 mg (1.64 μmol, 16%); LC/MS: Rt = 2.37 min (Vidac C₄, 50 - 90% MeCN, 15 min run); ESI-MS: *m/z* 1268.97 [M+H]⁺; HRMS Calcd for [C₆₆H₁₂₉N₁₁O₁₀S + H]⁺ 1268.97174, found 1268.97221.

P2X7, Cys((RS)-2,3-di(palimitoyloxy)-propyl)-Pra-Lys-Lys-Lys-Lys-NH₂

1.0 mg (0.78 μmol, 8%); LC/MS: Rt = 2.81 min (Vidac C₄, 50 - 90% MeCN, 15 min run); ESI-MS: *m/z* 1278.96 [M+H]⁺; HRMS Calcd for [C₆₇H₁₂₇N₁₁O₁₀S + H]⁺ 1278.95609, found 1278.95671.

P2X19, Cys((RS)-2,3-di(palimitoyloxy)-propyl)-Ala-Lys-Lys-Lys-Lys-NH₂

6.47 mg (5.15 μmol, 55%); LC/MS: Rt = 2.62 min (Vidac C₄, 50 - 90% MeCN, 15 min run); ESI-MS: *m/z* 1254.96 [M+H]⁺; HRMS Calcd for [C₆₅H₁₂₇N₁₁O₁₀S + H]⁺ 1254.95609, found 1254.95712.

P2X20, Cys((RS)-2,3-di(palimitoyloxy)-propyl)-CNAIa-Lys-Lys-Lys-Lys-NH₂

2.87 mg (2.24 μmol, 22%); LC/MS: Rt = 2.95 min (Vidac C₄, 50 - 90% MeCN, 15 min run); ESI-MS: *m/z* 1279.95 [M+H]⁺; HRMS Calcd for [C₆₆H₁₂₆N₁₂O₁₀S + H]⁺ 1279.95134, found 1279.95261.

P2X21, Cys((RS)-2,3-di(palimitoyloxy)-propyl)-Dap-Lys-Lys-Lys-Lys-NH₂

0.49 mg (0.38 μmol, 4%); LC/MS: Rt = 8.18 min (Vidac C₄, 10 - 90% MeCN, 15 min run); ESI-MS: *m/z* 1269.97 [M+H]⁺; HRMS Calcd for [C₆₅H₁₂₈N₁₂O₁₀S + H]²⁺ 635.48713, found 635.48679.

P2X23, Cys((RS)-2,3-di(palimitoyloxy)-propyl)-Phe-Lys-Lys-Lys-Lys-NH₂

1.79 mg (1.30 μmol, 13%); LC/MS: Rt = 3.38 min (Vidac C₄, 50 - 90% MeCN, 15 min run); ESI-MS: *m/z* 1330.99 [M+H]⁺; HRMS Calcd for [C₇₁H₁₃₁N₁₁O₁₀S + H]⁺ 1330.98739, found 1330.98781.

U14X2, 1-tetradecyl-urea-Cys((RS)-2,3-di(palimitoyloxy)-propyl)-Abu-Lys-Lys-Lys-Lys-NH₂

5.99 mg (3.97 μmol, 40%); LC/MS: Rt = 8.64 min (Vidac C₄, 50 - 90% MeCN, 15 min run); ESI-MS: *m/z* 1508.20 [M+H]⁺; HRMS Calcd for [C₈₁H₁₅₈N₁₂O₁₁S + H]⁺ 1508.19665, found 1508.19776.

U14X7, 1-tetradecyl-urea-Cys((RS)-2,3-di(palimitoyloxy)-propyl)-Pra-Lys-Lys-Lys-Lys-NH₂

1.38 mg (0.91 μmol, 9%); LC/MS: Rt = 8.10 min (Vidac C₄, 50 - 90% MeCN, 15 min run); ESI-MS: *m/z* 1518.18 [M+H]⁺; HRMS Calcd for [C₈₂H₁₅₆N₁₂O₁₁S + H]⁺ 1518.18100, found 1518.18239.

U14X19, 1-tetradecyl-urea-Cys((RS)-2,3-di(palimitoyloxy)-propyl)-Ala-Lys-Lys-Lys-Lys-NH₂

3.72 mg (2.50 μmol, 25%); LC/MS: Rt = 8.52 min (Vidac C₄, 50 - 90% MeCN, 15 min run); ESI-MS: *m/z* 1494.18 [M+H]⁺; HRMS Calcd for [C₈₀H₁₅₆N₁₂O₁₁S + H]⁺ 1494.18100, found 1494.18200.

U14X20, 1-tetradecyl-urea-Cys((RS)-2,3-di(palimitoyloxy)-propyl)-CNAIa-Lys-Lys-Lys-Lys-NH₂

3.3 mg (2.17 μmol, 22%); LC/MS: Rt = 8.10 min (Vidac C₄, 50 - 90% MeCN, 15 min run); ESI-MS: *m/z* 1519.18 [M+H]⁺; HRMS Calcd for [C₈₁H₁₅₅N₁₃O₁₁S + H]⁺ 1519.17625, found 1519.17775.

U14X21, 1-tetradecyl-urea-Cys((RS)-2,3-di(palimitoyloxy)-propyl)-Dap-Lys-Lys-Lys-Lys-NH₂

0.42 mg (0.28 μmol, 3%); LC/MS: Rt = 7.29 min (Vidac C₄, 50 - 90% MeCN, 15 min run); ESI-MS: *m/z* 1509.19 [M+H]⁺; HRMS Calcd for [C₈₀H₁₅₇N₁₃O₁₁S + H]²⁺ 755.09959, found 755.10017.

C12X2, Myristoyl-Cys((RS)-2,3-di(palimitoyloxy)-propyl)-Abu-Lys-Lys-Lys-Lys-NH₂

2.08 mg (1.41 μmol, 14%); LC/MS: Rt = 7.76 min (Vidac C₄, 50 - 90% MeCN, 15 min run); ESI-MS: *m/z* 1479.17 [M+H]⁺; HRMS Calcd for [C₈₀H₁₅₅N₁₁O₁₁S + H]⁺ 1479.17010, found 1479.17116.

C12X7, Myristoyl-Cys((RS)-2,3-di(palimitoyloxy)-propyl)-Pra-Lys-Lys-Lys-Lys-NH₂

2.08 mg (1.4 μmol, 14%); LC/MS: Rt = 7.90 min (Vidac C₄, 50 - 90% MeCN, 15 min run); ESI-MS: *m/z* 1489.15 [M+H]⁺; HRMS Calcd for [C₈₁H₁₅₃N₁₁O₁₁S + H]⁺ 1489.15545, found 1489.15512.

C12X19, Myristoyl-Cys((RS)-2,3-di(palimitoyloxy)-propyl)-Ala-Lys-Lys-Lys-Lys-NH₂

3.47 mg (2.37 μmol, 24%); LC/MS: Rt = 7.40 min (Vidac C₄, 50 - 90% MeCN, 15 min run); ESI-MS: *m/z* 1465.15 [M+H]⁺; HRMS Calcd for [C₇₉H₁₅₃N₁₁O₁₁S + H]⁺ 1465.15585, found 1465.15445.

C12X20, Myristoyl-Cys((RS)-2,3-di(palimitoyloxy)-propyl)-CNAIa-Lys-Lys-Lys-Lys-NH₂

1.50 mg (1.01 μmol, 10%); LC/MS: Rt = 7.69 min (Vidac C₄, 50 - 90% MeCN, 15 min run); ESI-MS: *m/z* 1490.15 [M+H]⁺; HRMS Calcd for [C₈₀H₁₅₂N₁₂O₁₁S + H]⁺ 1490.14970, found 1490.15061.

C12X21, Myristoyl-Cys((RS)-2,3-di(palimitoyloxy)-propyl)-Dap-Lys-Lys-Lys-Lys-NH₂

0.62 mg (0.42 μmol, 4%); LC/MS: Rt = 6.76 min (Vidac C₄, 50 - 90% MeCN, 15 min run); ESI-MS: *m/z* 1480.17 [M+H]⁺; HRMS Calcd for [C₇₉H₁₅₄N₁₂O₁₁S + H]⁺ 1480.16535, found 1480.16676.

U12X2, 1-dodecyl-urea-Cys((RS)-2,3-di(palimitoyloxy)-propyl)-Abu-Lys-Lys-Lys-Lys-NH₂

1.03 mg (0.70 μmol, 7%); LC/MS: Rt = 7.54 min (Vidac C₄, 50 - 90% MeCN, 15 min run); ESI-MS: *m/z* 1480.17 [M+H]⁺; HRMS Calcd for [C₇₉H₁₅₄N₁₂O₁₁S + H]⁺ 1480.16535, found 1480.16634.

U12X7, 1-dodecyl-urea-Cys((RS)-2,3-di(palimitoyloxy)-propyl)-Pra-Lys-Lys-Lys-Lys-NH₂

3.86 mg (2.99 μmol, 30%); LC/MS: Rt = 7.37 min (Vidac C₄, 50 - 90% MeCN, 15 min run); ESI-MS: *m/z* 1490.15 [M+H]⁺; HRMS Calcd for [C₈₀H₁₅₂N₁₂O₁₁S + H]⁺ 1490.14970, found 1490.15076.

U12X19, 1-dodecyl-urea-Cys((RS)-2,3-di(palimitoyloxy)-propyl)-Ala-Lys-Lys-Lys-Lys-NH₂

6.69 mg (4.57 μmol, 46%); LC/MS: Rt = 7.41 min (Vidac C₄, 50 - 90% MeCN, 15 min run); ESI-MS: *m/z* 1466.15 [M+H]⁺; HRMS Calcd for [C₇₈H₁₅₂N₁₂O₁₁S + H]⁺ 1466.14970, found 1466.15054.

U12X20, 1-dodecyl-urea-Cys((RS)-2,3-di(palimitoyloxy)-propyl)-CNAIa-Lys-Lys-Lys-Lys-NH₂

4.13 mg (2.77 μmol, 28%); LC/MS: Rt = 7.52 min (Vidac C₄, 50 - 90% MeCN, 15 min run); ESI-MS: *m/z* 1491.14 [M+H]⁺; HRMS Calcd for [C₇₉H₁₅₁N₁₃O₁₁S + H]⁺ 1491.14495, found 1491.14578.

U12X21, 1-dodecyl-urea-Cys((RS)-2,3-di(palimitoyloxy)-propyl)-Dap-Lys-Lys-Lys-Lys-NH₂

0.41mg (0.28 μmol, 3%); LC/MS: Rt = 6.88 min (Vidac C₄, 50 - 90% MeCN, 15 min run); ESI-MS: *m/z* 1481.16 [M+H]⁺; HRMS Calcd for [C₇₉H₁₅₄N₁₂O₁₁S + H]⁺ 1481.16060, found 1481.16281.

C10X2, Lauroyl-Cys((RS)-2,3-di(palimitoyloxy)-propyl)-Abu-Lys-Lys-Lys-Lys-NH₂

2.43 mg (1.68 μmol, 17%); LC/MS: Rt = 7.05 min (Vidac C₄, 50 - 90% MeCN, 15 min run); ESI-MS: *m/z* 1451.14 [M+H]⁺; HRMS Calcd for [C₇₈H₁₅₁N₁₁O₁₁S + H]⁺ 1451.13880, found 1451962.

C10X7, Lauroyl-Cys((RS)-2,3-di(palimitoyloxy)-propyl)-Pra-Lys-Lys-Lys-Lys-NH₂

2.28 mg (1.56 μmol, 16%); LC/MS: Rt = 7.14 min (Vidac C₄, 50 - 90% MeCN, 15 min run); ESI-MS: *m/z* 1461.12 [M+H]⁺; HRMS Calcd for [C₇₉H₁₄₉N₁₁O₁₁S + H]⁺ 1461.12315, found 1461.12399.

C10X19, Lauroyl-Cys((RS)-2,3-di(palimitoyloxy)-propyl)-Ala-Lys-Lys-Lys-Lys-NH₂

4.96 mg (3.45 μmol, 35%); LC/MS: Rt = 6.68 min (Vidac C₄, 50 - 90% MeCN, 15 min run); ESI-MS: *m/z* 1437.12 [M+H]⁺; HRMS Calcd for [C₇₇H₁₄₉N₁₁O₁₁S + H]⁺ 1437.12315, found 1437.12394.

C10X20, Lauroyl-Cys((RS)-2,3-di(palimitoyloxy)-propyl)-CNAIa-Lys-Lys-Lys-Lys-NH₂

2.28 mg (1.56 μmol, 16%); LC/MS: Rt = 7.09 min (Vidac C₄, 50 - 90% MeCN, 15 min run); ESI-MS: *m/z* 1462.12 [M+H]⁺; HRMS Calcd for [C₇₈H₁₄₈N₁₂O₁₁S + H]⁺ 1462.11840, found 1462.11993.

C10X21, Lauroyl-Cys((RS)-2,3-di(palimitoyloxy)-propyl)-Dap-Lys-Lys-Lys-Lys-NH₂

0.38mg (0.26 μmol, 3%); LC/MS: Rt = 6.45 min (Vidac C₄, 50 - 90% MeCN, 15 min run); ESI-MS: *m/z* 1452.13 [M+H]⁺; HRMS Calcd for [C₇₇H₁₅₀N₁₂O₁₁S + H]²⁺ 726.57066, found 726.57059.

U10X2, 1-decyl-urea-Cys((RS)-2,3-di(palimitoyloxy)-propyl)-Abu-Lys-Lys-Lys-Lys-NH₂

4.47 mg (3.08 μmol, 31%); LC/MS: Rt = 6.93 min (Vidac C₄, 50 - 90% MeCN, 15 min run); ESI-MS: *m/z* 1452.13 [M+H]⁺; HRMS Calcd for [C₇₇H₁₅₀N₁₂O₁₁S + H]⁺ 1452.13405, found 1452.13487

U10X7, 1-decyl-urea-Cys((RS)-2,3-di(palimitoyloxy)-propyl)-Pra-Lys-Lys-Lys-Lys-NH₂

3.94 mg (2.69 μmol, 27%); LC/MS: Rt = 6.69 min (Vidac C₄, 50 - 90% MeCN, 15 min run); ESI-MS: *m/z* 1462.12 [M+H]⁺; HRMS Calcd for [C₇₈H₁₄₈N₁₂O₁₁S + H]⁺ 1462.11840, found 1462.11892.

U10X19, 1-decyl-urea-Cys((RS)-2,3-di(palimitoyloxy)-propyl)-Ala-Lys-Lys-Lys-Lys-NH₂

3.22 mg (2.24 μmol, 22%); LC/MS: Rt = 6.73 min (Vidac C₄, 50 - 90% MeCN, 15 min run); ESI-MS: *m/z* 1438.12 [M+H]⁺; HRMS Calcd for [C₇₆H₁₄₈N₁₂O₁₁S + H]⁺ 1438.11840, found 1438.11901.

U40 U10X20, 1-decyl-urea-Cys((RS)-2,3-di(palimitoyloxy)-propyl)-CNAIa-Lys-Lys-Lys-Lys-NH₂

1.84 mg (1.26 μmol, 13%); LC/MS: Rt = 6.93 min (Vidac C₄, 50 - 90% MeCN, 15 min run); ESI-MS: *m/z* 1463.11 [M+H]⁺; HRMS Calcd for [C₇₇H₁₄₇N₁₃O₁₁S + H]⁺ 1463.11365, found 1463.11459.

U10X21, 1-decyl-urea-Cys((RS)-2,3-di(palimitoyloxy)-propyl)-Dap-Lys-Lys-Lys-Lys-NH₂

0.45 mg (0.31 μmol, 3%); LC/MS: Rt = 6.46 min (Vidac C₄, 50 - 90% MeCN, 15 min run); ESI-MS: *m/z* 1454.13 [M+H]⁺; HRMS Calcd for [C₇₆H₁₄₉N₁₃O₁₁S + H]²⁺ 722.06829, found 722.06834.

U14X1-DEVA₅K, *1-tetradecyl-urea-Cys((RS)-2,3-di(palimitoyloxy)-propyl)-Ser-Lys-Lys-Lys-Lys-Asp-Glu-Val-Ser-Gly-Leu-Glu-Gln-Leu-Glu-Ser-Ile-Ile-Asn-Phe-Glu-Lys-Leu-Ala-Ala-Ala-Ala-Lys-NH₂*
6.71 mg (1.66 μmol, 8%); LC/MS: Rt = 9.82 min (Vidac C₄, 10 - 90% MeCN, 15 min run); ESI-MS: *m/z* 4039.50 [M+H]⁺; HRMS Calcd for [C₁₉₂H₃₃₈N₄₀O₅₀S + H]²⁺ 2020.25296, found 2020.24719.

U14X2-DEVA₅K, *1-tetradecyl-urea-Cys((RS)-2,3-di(palimitoyloxy)-propyl)-Abu-Lys-Lys-Lys-Lys-Asp-Glu-Val-Ser-Gly-Leu-Glu-Gln-Leu-Glu-Ser-Ile-Ile-Asn-Phe-Glu-Lys-Leu-Ala-Ala-Ala-Ala-Lys-NH₂*
3.48 mg (0.86 μmol, 3%); LC/MS: Rt = 6.74 min (Vidac C₄, 50 - 90% MeCN, 15 min run); ESI-MS: *m/z* 4037.52 [M+H]⁺; HRMS Calcd for [C₁₉₃H₃₄₀N₄₀O₄₉S + H]³⁺ 1346.51131, found 1346.51212

U12X2-DEVA₅K, *1-dodecyl-urea-Cys((RS)-2,3-di(palimitoyloxy)-propyl)-Abu-Lys-Lys-Lys-Lys-Asp-Glu-Val-Ser-Gly-Leu-Glu-Gln-Leu-Glu-Ser-Ile-Ile-Asn-Phe-Glu-Lys-Leu-Ala-Ala-Ala-Ala-Lys-NH₂*
5.08 mg (1.3 μmol, 5%); LC/MS: Rt = 5.97 min (Vidac C₄, 50 - 90% MeCN, 15 min run); ESI-MS: *m/z* 4008.48 [M+H]⁺; HRMS Calcd for [C₁₉₁H₃₃₆N₄₀O₄₉S + H]³⁺ 1337.16754, found 1337.16878.

P2X2-DEVA₅K, *Cys((RS)-2,3-di(palimitoyloxy)-propyl)-Abu-Lys-Lys-Lys-Lys-Asp-Glu-Val-Ser-Gly-Leu-Glu-Gln-Leu-Glu-Ser-Ile-Ile-Asn-Phe-Glu-Lys-Leu-Ala-Ala-Ala-Ala-Lys-NH₂*
9.79 mg (2.6 μmol, 10%); LC/MS: Rt = 1.68 min (Vidac C₄, 50 - 90% MeCN, 15 min run); ESI-MS: *m/z* 3797.29 [M+H]⁺; HRMS Calcd for [C₁₇₈H₃₁₁N₃₉O₄₈S + H]³⁺ 1266.76965, found 1266.77147.

C14X2-DEVA₅K, *Palmitoyl-Cys((RS)-2,3-di(palimitoyloxy)-propyl)-Abu-Lys-Lys-Lys-Lys-Asp-Glu-Val-Ser-Gly-Leu-Glu-Gln-Leu-Glu-Ser-Ile-Ile-Asn-Phe-Glu-Lys-Leu-Ala-Ala-Ala-Ala-Lys-NH₂*
3.29 mg (0.81 μmol, 3.3 %); LC/MS: Rt = 7.07 min (Vidac C₄, 50 - 90% MeCN, 15 min run); ESI-MS: *m/z* 4036.53 [M+H]⁺; HRMS Calcd for [C₁₉₄H₃₄₁N₃₉O₄₉S + H]³⁺ 1346.17957, found 1346.18051.

7.3 References and notes

- (1) Fuchs, T., Schmidt, R. R., *Synthesis*, **1998**, 753-758.
- (2) Malkinson, J. P., Falconer, R. A., Toth, I., *J Org Chem*, **2000**, *65*, 5249-5252.
- (3) Coulombe, F., Divangahi, M., Veyrier, F., de Leseleuc, L., Gleason, J. L., Yang, Y., Kelliher, M. A., Pandey, A. K., Sasseti, C. M., Reed, M. B., Behr, M. A., *J Exp Med*, **2009**, *206*, 1709-1716.
- (4) Renaudet, O., BenMohamed, L., Dasgupta, G., Bettahi, I., Dumy, P., *ChemMedChem*, **2008**, *3*, 737-741.
- (5) Cai, H., Huang, Z. H., Shi, L., Zhao, Y. F., Kunz, H., Li, Y. M., *Chemistry*, **2011**, *17*, 6396-6406.
- (6) Fujimoto, Y., Konishi, Y., Kubo, O., Hasegawa, M., Inohara, N., Fukase, K., *Tetrahedron Lett*, **2009**, *50*, 3631-3634.
- (7) Inamura, S., Fujimoto, Y., Kawasaki, A., Shiokawa, Z., Woelk, E., Heine, H., Lindner, B., Inohara, N., Kusumoto, S., Fukase, K., *Org Biomol Chem*, **2006**, *4*, 232-242.
- (8) Lee, J., Tattoli, I., Wojtal, K. A., Vavricka, S. R., Philpott, D. J., Girardin, S. E., *J Biol Chem*, **2009**, *284*, 23818-23829.
- (9) Agnihotri, G., Ukani, R., Malladi, S. S., Warshakoon, H. J., Balakrishna, R., Wang, X., David, S. A., *J Med Chem*, **2011**, *54*, 1490-1510.
- (10) Buwitt-Beckmann, U., Heine, H., Wiesmuller, K. H., Jung, G., Brock, R., Akira, S., Ulmer, A. J., *Eur J Immunol*, **2005**, *35*, 282-289.
- (11) Buwitt-Beckmann, U., Heine, H., Wiesmuller, K. H., Jung, G., Brock, R., Ulmer, A. J., *Febs J*, **2005**, *272*, 6354-6364.
- (12) Okusawa, T., Fujita, M., Nakamura, J., Into, T., Yasuda, M., Yoshimura, A., Hara, Y., Hasebe, A., Golenbock, D. T., Morita, M., Kuroki, Y., Ogawa, T., Shibata, K., *Infect Immun*, **2004**, *72*, 1657-1665.
- (13) Ghosh, A., E., F., *Tetrahedron Lett*, **2000**, *41*, 165-168.